Journal of Applied Mechanics and Technical Physics, Vol. 40, No. 1, 1999

STRUCTURE OF STRATIFIED FLOW AROUND A CYLINDER AT LOW INTERNAL FROUDE NUMBER

V. V. Mitkin and Yu. D. Chashechkin

UDC 532.5.013.4:551.465.41

The flow pattern around a horizontal cylinder towed at constant velocity in a continuously stratified fluid is visualized by the shadow method. The velocities in the leading flow disturbance, i.e., in the flow-blocking region ahead of the cylinder, are presented. In the body wake, a new class of small-size structures in the density gradient field is revealed against the background of a smooth velocity profile. The evolution of the flow pattern with variation of the parameters of body motion is studied.

Measurements using highly sensitive devices, which have become regular since the late 1960s, have revealed a large number of periodic finely structured features in both vertical profiles and horizontal sections of physical fields of the ocean and atmosphere. In these fields, relatively thick uniform layers are separated by thin high-gradient interlayers and fronts. Specific internal waves and local small-scale vortices that can be generated in the interlayers constitute wave-vortex turbulence. This turbulence was observed in summer thermoclines [1] and deeper in the ocean. However, data of full-scale observations were insufficient to determine the mechanisms of formation and preservation of discontinuities in the density and its gradients that counterbalance the smoothing effect of diffusion processes and to estimate the influence of perturbations of the density field on the flow stability and transport of active or passive additives.

It turned out that changes in continuous stratification and the stability of structures that arise are conveniently studied using two- and three-dimensional wake flows [2–5]. Contact measurements showed that in the high-gradient interlayers that bound a two-dimensional laminar wake, the initial density gradient increases by a factor of 10–150 [4]. In this wake, along with large-scale vortices, small-scale vortices can be observed, with the sizes dependent on the interlayer thickness. Examples of various types of instability of wake flow that result in the formation of "spear-shaped" structures in a wake and wave-vortex surfs and high-gradient interlayers downstream of dangling vortices in the body wake are reported in [5].

Discontinuities in the density and its gradient are an important part of the wake flow in an initially continuously stratified fluid. They bound the regions of existence of large-scale phenomena such as attached internal waves, vortices, and their systems (dangling or submerged in the wake) and influence transport of active and passive additives and propagation of electromagnetic and acoustic waves.

The purpose of this work was to study one type of fine structures that are related to the previously unstudied flow instability in the immediate vicinity of a body moving with constant velocity in a deep, continuously stratified fluid at rest.

Determining Parameters. The complete system of fluid-dynamic equations describing nonuniform fluid flow around an obstacle includes equations of state, continuity, and conservation of salt and momentum, and boundary conditions (conditions of attachment for the velocity and nonpenetration for the material on the solid surface).

A stratified fluid is a nonequilibrium medium in which diffusion-induced compensating flows originate on the inclined impermeable boundaries blocking the molecular flow of a stratifying component even in the

Institute of Mechanics Problems, Moscow 117526. Translated from Prikladnaya Mekhanika i Tekhnicheskaya Fizika, Vol. 40, No. 1, pp. 80–88, January–February, 1999. Original article submitted December 3, 1996; revision submitted March 19, 1997.

0021-8944/99/4001-0069 $22.00

absence of external disturbances [6]. These boundary flows exhibit different scales of variation in velocity and density (salinity), whose ratio is independent of time and is determined by the Schmidt number. These features remain after separation of the split boundary layer from the body. Accordingly, both in the immediate vicinity of and far away from the body there are flow regions (high-gradient interlayers) whose dynamics depends greatly on the molecular properties of the medium.

Stratified flow around an obstacle is determined by the following dimensional parameters: the density ρ_0 and its gradient $d\rho_0/dz$, the kinematic viscosity ν and diffusivity k_s of the salt, the velocity U and dimensions D of the body, and the free-fall acceleration g. From a methodical viewpoint, it makes sense to use uniform quantities, which, in our case, have the dimension of length. This is not a mere formality: each scale can be put into correspondence with a certain flow structural element (or an element of the problem's geometry).

The basic scales in the present approach are the following: the buoyancy scale $\Lambda = |d(\ln \rho_0)/dz|^{-1}$ (the z axis is vertical), the body dimension (e.g., the diameter of the cylinder D), the wavelength of an attached internal wave $\lambda = UT_b = 2\pi U/N$, where $T_b = 2\pi/N = 2\pi\sqrt{\Lambda/g}$ is the buoyancy period (N is the frequency), and the thicknesses of the velocity ($\delta_\nu = \nu/U$) and density ($\delta_\rho = k_s/U$) boundary layers. These scales are used to construct a denumerable set of combined scales $L_c = \sqrt[a+b+\ldots]{L_1^a L_2^b \ldots}$. These derived scales are of different natures; some of them characterize the geometry of the process (including the dimensions of the main structural elements, among which is the so-called viscous wave scale $L_\nu = \sqrt[3]{\Lambda\lambda\delta_\nu} = \sqrt[3]{g\nu}/N$, related to the modal structure of harmonic internal waves and the dimension of vortices in the wake past the cylinder or the thickness of their boundaries [3]), and others reflect translational properties or the phenomena caused by the dissipative factors: the viscosity ($\delta_N = \sqrt{\nu/N}$) and diffusion ($\delta_d = \sqrt{k_s/N}$). Of derived scales that depend on several kinetic coefficients, one can distinguish the scale $L_w = \sqrt[4]{\nu k_s/N^2}$, which characterizes internal waves of zero frequency (dissipative-gravity waves in problems on convection [7]).

According to this approach, the traditional dimensional parameters in the problem of interest are defined as the ratios of basic scales. For example, the Reynolds number $\mathrm{Re} = D/\delta_\nu = UD/\nu$ is the ratio of the typical body dimension to the characteristic length of the viscous boundary-layer. Similarly, the Peclet number $\mathrm{Pe} = D/\delta_\rho = UD/k_s$ is the ratio of the typical body dimension to the thickness of the density boundary layer, the internal Froude number $\mathrm{Fr} = \lambda/2\pi D = U/ND$ is the ratio of the wavelength of an attached internal wave to the typical body dimension, and $C = \Lambda/D$ is the ratio of the scales. The Schmidt number is ratio of Pe to Re: $\mathrm{Sc} = \mathrm{Pe}/\mathrm{Re}$.

In a series of tests performed, the values of the main determining parameters were chosen from the condition of stability of the known flow structural elements (leading disturbance, body wake, and attached internal waves). Nevertheless, there are combinations of parameters that give rise to special small-scale flow structural elements whose degree of distinctness changes smoothly during monotonic variation of one of the dimensional parameters (flow velocity or body diameter). Analysis of our previous studies [3–5] shows that these phenomena occur at moderate Reynolds numbers ($\mathrm{Re} < 100$), at which the flow is stable against large-scale vortex disturbances ($\mathrm{Fr} < 0.1$). In this connection, the experimental procedure was chosen from the condition of simultaneous visualization of large- and small-scale structural elements. The Maksutov method with a vertical illumination slit and a flat or thread-like stop aperture is most conveniently used to solve this problem.

Experimental Procedure. The tests were carried out in a 240 × 40 × 60 cm tank with transparent walls. The tank was filled with a linearly stratified aqueous solution of sodium salt by the method of continuous displacement. Prior to each test, the buoyancy period T_b was measured by an electric conductivity meter with an accuracy within 5%. In the tests performed, the period was 6.8 sec, gradually increasing to 7.7 sec owing to natural liquid diffusion and mixing.

The flow pattern past a horizontal cylinder of diameter D = 2.5, 5.0, and 7.6 cm was studied. The cylinder was towed with constant velocity in the central part of the tank. It was fastened with thin knives to a carriage which was moved along the guides with a velocity U = 0.024–1.0 cm/sec (increment ΔU = 0.02 cm/sec and accuracy of velocity determination better than 5%). Prior to each test, the cylinder was placed at the edge wall of the basin. The experimental conditions (C = 150–560, Fr = 0.004–0.044, and Re = 16.5–167)

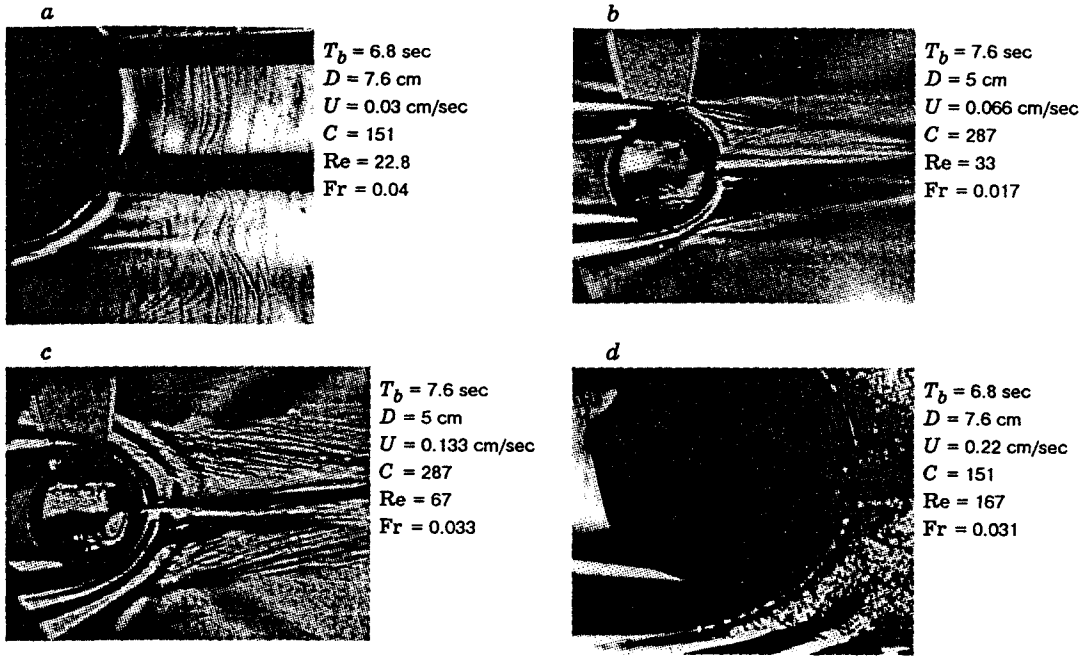

Fig. 1. Shadowgraphs of the fine structures generated by the instability of the density boundary layer on the cylinder in a continuously stratified fluid.

correspond to the laminar wake in the flow diagram in [2, 3, 8].

Flow visualization was carried out by an IAB-458 shadow device by two modifications of the Maksutov method: "vertical slit–knife" or "slit–thread in a focus." The first and second methods visualize the horizontal component and absolute value of the refraction index, respectively. The density markers were gas bubbles rising up to the surface or sugar crystals falling in the fluid. The typical lifetime of a marker was 40–100 sec, and its thickness was smaller than 1 mm.

Main Results. Typical shadowgraphs of the stratified flow around the horizontal cylinder (the "slit–knife" method) are shown in Fig. 1. In all cases, the body moves from right to left.

Previous experiments [4] showed that the laminar regime, the boundaries of the blocked-fluid region ahead of the body, a high-gradient layer of the density body wake, and just one internal wave leading the body are clearly seen. In the present series of tests, the experimental conditions of [4] were reproduced and used as initial conditions for the formation of high-gradient interlayers. For $T_b = 7.6$, $D = 5$ cm, $U = 0.033$ cm/sec, $C = 287$, Re $= 16.5$, and Fr $= 0.008$, the angle of approach of the blocked-liquid boundary reckoned from the leading stagnation point $\varphi_a = 55°$, and the angle of interlayer departure in the wake past the body, reckoned from the rear stagnation point $\varphi_s = 40°$. From the measured displacement of the density marker, it was found that the maximum velocity at the center of the wake exceeds the body velocity because of a certain general contraction of the wake flow. The thickness of the velocity shear layer at the boundary of the wake is $\delta_u \approx 1$ cm, and the maximum shear frequency is $\omega_u = du/dz = 0.053$ sec^{-1}, i.e., it is the same order of magnitude as the shear frequency in front of the body. The Richardson local gradient number determined from the undisturbed buoyancy frequency is $\mathrm{Ri}_0 = N_0^2/\omega_u^2 = 290 \gg 1$, and no other structural nonuniformities are present in the flow except for the nearly horizontal high-gradient layers outlining the density wake.

With increase in the diameter of the body and decrease in the Froude number, isolated discontinuities in the density gradient field appear in the wake past the body. They have the shape of short folds of length $l \sim 3.5$ cm and thickness $\delta \approx 0.1$ cm spaced 4 cm apart from the wake axis (Fig. 1a). The departure angle of the high-gradient layers of the density wake reckoned from the rear stagnation point is 35°, whereas the departure angle of the small-scale inhomogeneities is appreciably higher: $\varphi_i = 70°$. Two groups of markers can be seen. One of them was created before the body passed through the field of vision, and the other after that.

TABLE 1

U, cm/sec	Re	Fr	φ_i, deg
0.1	50.0	0.025	85
0.133	67.0	0.033	82
0.175	87.5	0.042	76

They visualize a comparatively smooth velocity profile, whose typical shear layer is at least 18 times thicker ($\delta_u \approx 1.8$ cm) than the high-gradient interlayer in the density field. The Richardson local number determined from the undisturbed buoyancy frequency is Ri = 740, and the condition for hydrodynamic instability (the Miles–Howard criterion $\mathrm{Ri}_{cr} < 0.25$ [9]) is not fulfilled for the flow region where the small-scale structure of the density gradient field is observed. The attached internal waves (of length $\lambda = 0.2$ cm in this regime) freely pass through all these density disturbances and get attached to the high-gradient periphery of the density wake.

With increase in the body velocity, accompanied by approach of the density layers and formation of a centered wake, the density field shows several new microfeatures (Fig. 1b), namely, inclined "folds" of thickness $\delta \sim 0.5$ cm with a departure angle $\varphi_i = 85°$, and elongated hyperbola-shaped folds taking their origin in the separation region of the density wake.

Outside the field of internal waves, two classes of inhomogeneities can be distinguished: smoother inhomogeneities, with thickness $\delta = 0.2$ cm and length $l = 3.3$ cm inclined at an angle to the direction of motion, and more gently sloping inhomogeneities of thickness $\delta = 0.3$ cm in the right part of the shadowgraph. The shape of these folds indicates the existence of a vertical (vortex) velocity component in the wake, with an average value of about 10% of the body velocity. The location of the folds relative to the body is stationary. The geometry of the folds in the region of their separation indicates the existence of a rather restricted region of their formation near the body surface, with an angular position of 85° from the rear stagnation point. Fine folds of a similar structure were observed in other tests over a rather wide range of parameters listed in Table 1 ($T_b = 7.6$ sec, $D = 5$ cm, and $C = 287$).

At the upper boundary of the density wake, a nearly horizontal ultra-thin interlayer (as thin as 0.1 cm) is observed. The pattern of disturbances near the body shows that a similar interlayer bounds the density wake from below, where it is not shadowed by larger flow inhomogeneities.

The typical transverse size of the folds ($\delta \sim 0.2$ cm) is well below all characteristic scales of the problem, except for the thickness of the density boundary layer $\delta_\rho = k_s/U$ and the diffusion scale $\delta_d = \sqrt{k_s/N}$.

With further increase in the velocity, both the length and amplitude of the attached internal waves grow, and the shadow method permits visualization of three waves (Fig. 1c). Owing to the variation in the density field, a high-gradient interlayer that separates the first attached internal wave from the obstacle forms along the cylinder surface. Inside the interlayer, microscale inhomogeneities can be seen. Simultaneously, the degree of distinctness of the fine structure occupying the entire wake past the cylinder increases.

The location and shape of particular elements longer than 5 cm allow one to distinguish three groups of small-scale inhomogeneities: elliptical irregular structures in the bottom part of the body, linear structures in the central part of the wake, and diffusion-induced folds on the flow periphery. The central part of the wake in this regime is practically free of inhomogeneities.

The elliptical inhomogeneities have minimum thickness ($\delta \sim 0.1$ cm), and their length increases with distance from the bottom part of the body. The inhomogeneities adjoining this region are thin strips of length $l \sim 4$–5 cm and thickness $\delta \sim 0.1$–0.2 cm inclined at an angle $\alpha \approx 15°$ to the plane of motion of the body center. The inclined linear swirls ($\alpha \approx 7°$) are somewhat thicker and as long as 6 cm. The third group of strips is caused by laminarization of the periphery of the wake flow.

These small-scale inhomogeneities do not change the general density distribution, since the phase surfaces of the internal waves pass through these structures without being disturbed. The extension of the region of small-scale disturbances behind the body is at least 40 cm, and the lifetime of individual elements

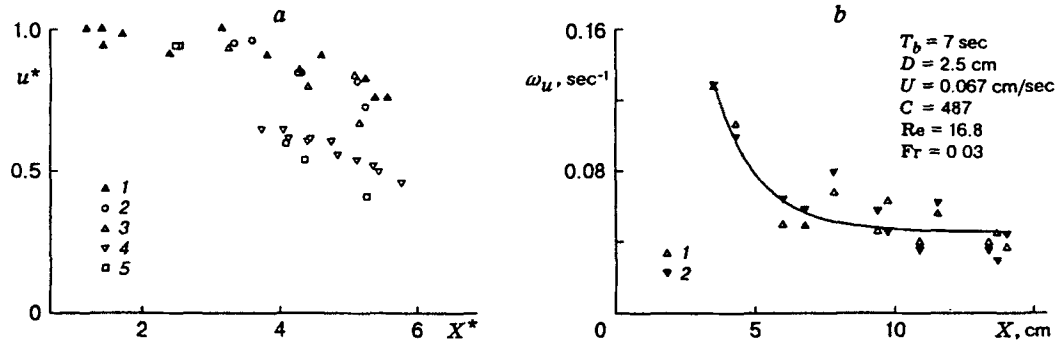

Fig. 2. Lengthwise distribution of the maximum flow velocity (a) and the velocity shear frequency (b) in the leading disturbance in front of the body for the upper and lower parts of the disturbance (points 1 and 2). The curve is an extrapolation of the experimental data.

of the structure exceeds 300 sec, which is in line with the estimated diffusion time $t = \delta^2/k_s \sim 700$ sec.

With further increase in the body diameter, when the Reynolds number rises and the Prandtl number decreases, the density disturbances in the bottom part of the flow show a pronounced three-dimensional structure (Fig. 1d). The typical transverse and longitudinal scales of the structural inhomogeneity are both 0.15 cm. The maximum departure angle of the structured flow is $\varphi_i \approx 95°$.

The density disturbances near the body are so strong that they give rise to additional extrema in the shadowgraphs of the field of internal waves (in the shadowgraphs shown in Fig. 1d, they correspond to the dark band separated by a thin 0.3-cm-thick layer from the first crest of the internal wave and the body surface; the angular position of its leading edge is $\varphi = 115°$ from the rear stagnation point). These wavelike disturbances penetrate deep into the zone of small-scale fluctuations, and they are deflected by the shear flow from the body surface only near the top boundary of the centered density wake. The length of the attached internal wave in this regime is $\lambda \approx 1.5$ cm, which agrees well with the value $\lambda = UT_b$ given by the linear theory.

Visualization of the entire flow pattern shows the phase surfaces of the second and third internal waves only at the outer boundary and in the region of small-scale fluctuations, where their canonical shape (an arc of a circle) is distorted because of entrainment in the wake flow. Owing to the Doppler effect, they even change their curvature sign near the wake core [the curvature radius of a regular internal wave $R^+ = 4.2$ cm, and the imaginary center is inside the body; the curvature radius of the wave-like disturbance adjacent to the density wake is $R^- = -1.25$ cm (Fig. 1d)].

This type of structure shows a pronounced dimensional character. If the body diameter is smaller than the viscous wave scale ($D < L_\nu$), the above interlayers are not observed in the density gradient field (and in the field of the visualized parameter, the gradient of the refractory index, related to the density gradient by a linear expression). In particular, at $T_b = 6.9$ sec, $D = 2.5$ cm, $U = 0.1$ cm/sec, $C = 474$, $D/L_\nu = 1$, Re = 25, and Fr = 0.044, the wave pattern is regular, and small-scale structural elements are not observed, although the dynamic parameters here (Re and Pr numbers) are intermediate between the values corresponding to the conditions of Fig. 1.

Figure 2a shows results of processing images of density markers in front of a cylinder of diameter 2.5 cm obtained in a series of tests for the values of the determining parameters listed in Table 2.

In all cases, the maximum flow velocity in front of the body decreases monotonically with distance by the law $u^* = b - aX^*$ ($u^* = u/U$ and $X^* = X/D$, where X is the horizontal coordinate reckoned from the leading edge of the body); the coefficient a increases monotonically with increase in the velocity of the body. Extrapolating the dependences obtained, one can see that, according to the experimental procedure of [7], where $u^*(L_b^*) = 0.2$ and $L_b^* = L_b/D$, the boundary of the blocked fluid is at distances $L_b^* = 48$, 27,

TABLE 2

Test	T_b, sec	U, cm/sec	C	Re	Fr
1	7.0	0.067	487	16.8	0.03
2	6.9	0.0175	473	44.0	0.077
3	6.9	0.210	473	53.0	0.097
4	7.5	0.235	560	59.0	0.11
5	7.2	0.4	515	100	0.18

26, 21, and 15 cm from the leading edge of the body. This contradicts the results of [8], according to which, $L_b^* = \mathrm{Re}/(300\,\mathrm{Fr}^2)$, and for the values listed in Table 2, the boundary is at distances $L_b^* = 155$, 61, 50, 41, and 25 cm.

The liquid particles located in front of the obstacle near the trajectory of its center do not have sufficient energy to move along the vertical as far as the body radius [10]. Owing to the accumulation of the liquid near the horizon of motion of body's center, the initial density gradient in front of the body decreases. In some calculations, the leading disturbance in a continuously stratified fluid has the shape of a train of solitary waves. A similar flow pattern was observed in experiments with two-layered fluids, both miscible and immiscible [11, 12]. In these tests, a nonstationary train of waves was formed when the body velocity was close to the critical velocity of an internal mode.

In the continuously stratified fluid, only monotonic leading disturbances were observed. All the marker profiles were rather smooth, with minima and maxima lying at the phase surfaces of the leading nonstationary internal waves.

From the velocity profiles constructed from the displacements of density markers, the maximum shear frequency in the boundary-layer region at the outer boundary of the blocked fluid was determined as a function of the distance from the center of the body (Fig. 2b) for the upper and lower parts of the leading disturbance (points 1 and 2); the graph also shows the extrapolating curve $\omega_u = 0.046 + 0.08\exp(-(X-3.6)/1.6)$, where the quantities entering the exponent are measured in centimeters. The more abrupt decrease in the velocity shear frequency compared to the decrease in the maximum fluid velocity in front of the body is related to the increase in the separation between the extrema in the velocity profile due to expansion of the leading disturbance with distance from the source. In all cases, the Richardson local gradient numbers $\mathrm{Ri} = N^2/(\omega_u^2)^2$ in front of the body far exceed the critical value [9] ($\mathrm{Ri} > 15$) and shear instability does not develop.

Discussion. The experiments described show that in the stratified flow past a cylinder over wide ranges of the determining parameters ($\mathrm{Fr} = 0.004$–0.044, $\mathrm{Re} = 33$–167, and $C = 151$–287), reconstruction of the stratified flow is observed, which is accompanied by the development of a special type of small-scale instability at high Richardson gradient numbers ($\mathrm{Ri}_0 \gg 1$). In the flow pattern around the cylinder, strong fluctuations of the gradient of the refractive index (and, hence, density) are observed against the background of a smooth velocity profile (regime of "structural" turbulence).

Physically, this flow pattern may be caused by instability of the most small-scale structural element of the stratified flow around the cylinder — the density boundary layer [4, 6, 7]. This layer forms owing to blocking of the molecular flow of the stratifying component by the impermeable body. The thickness of the density boundary layer (between the blocked fluid and the outside flow ahead of the body and between the flow elements in the convergent zone in the vicinity of the separation point of the density wake behind the body) is determined by the diffusivity and the buoyancy frequency [6, 7].

Thin high-gradient interlayers were previously observed at the outer boundary of a density wake [4]. The shadowgraphs in Fig. 1 indicate that such interlayers form in the vicinity of the body outside the density wake. High-gradient folds directed along the average velocity vector arise in the wake flow when the separation point begins to oscillate.

Instability of the entire density boundary layer results in the formation of a finely structured flow pattern, which is transferred as a "frozen" one by the external flow. Small-scale inhomogeneities slowly transform and disintegrate under the action of buoyancy forces, which act to drive each structural element

to the neutral buoyancy horizon, and molecular diffusion, which diminishes the differences in density and the degree of contrast of the shadowgraphs.

The slow increase in the minimum thickness of the small-scale structural elements along the wake with distance from the body (or with increase in their lifetime) indicates the important role of deformation (elongation of liquid particles along the flow) in the evolution of the fine structure of the wake flow and direct interaction of finely structured flow elements with internal waves.

The microscale instability is of a pronounced dimensional character. It is not observed near obstacles of small diameter even when the dynamic characteristics of the process (Reynolds and Froude numbers) are in the region of existence of the instability, and this is indicative of incompleteness of the traditional parametrization of this class of flows [2, 8]. Taking into account the features of transport of additives by stratified flow, one can state that this instability and the associated instability-induced stratification structures should influence both the rapid (ultrarapid) propagation of passive elements along the interlayers and lines of intersection of the interlayers and formation of empty regions (voids) inside isolated vortices.

The reproducibility of the geometry and subtle details of inhomogeneities of this type (observed in many experiments for various stratifications around cylinders of various dimensions) and the continuous dependence of their main properties (degree of distinctness, geometry and dimensions of the occupied region, and lifetime) on the flow external parameters indicate that the special class of small-scale structures should be included in the set of identification criteria in constructing diagrams of stratified flows around two-dimensional obstacles and the properties of these structures should be studied more thoroughly. The effects described above can also be observed under natural conditions, in the ocean and atmosphere, where obstacles are rather extended and the region of interaction of incoming stratified flow with relief is rather extended.

This work was supported by the Russian Foundation for Fundamental Research (Grant No. 96-05-64004) and the Ministry of Science and Technical Policy of the Russian Federation (a grant in support of Russia's unique apparatus).

REFERENCES

1. J. D. Woods, "Wave-induced shear in summer thermoclines," *J. Fluid Mech.*, **32**, No. 4, 791–800 (1968).
2. Xu Yunxie, H. J. S. Fernando, and D. L. Boyer, "Turbulent wakes of stratified flow past a cylinder," *Phys. Fluids*, **7**, No. 9, 2243–2255 (1995).
3. Yu. D. Chashechkin and I. V. Voeikov, "Vortices past a cylinder in a continuously stratified fluid," *Izv. Ross. Akad. Nauk, Fiz. Atmos. Okeana*, **29**, No. 6, 821–830 (1993).
4. I. V. Voeikov and Yu. D. Chashechkin, "Formation of discontinuities in the wake past a cylinder in a stratified fluid," *Izv. Ross. Akad. Nauk, Mekh. Zhidk. Gaza*, No. 1, 20–26 (1993).
5. V. I. Voeikov, V. E. Prokhorov, and Yu. D. Chashechkin, "Microscale instability in a continuously stratified fluid," *Izv. Ross. Akad. Nauk, Mekh. Zhidk. Gaza*, No. 3, 3–10 (1998).
6. V. G. Baidulov and Yu. D. Chashechkin, "Effect of diffusion on boundary flows in a continuously stratified fluid," *Izv. Ross. Akad. Nauk, Mekh. Zhidk. Gaza*, **29**, No. 5, 666–672 (1993).
7. A. V. Kistovich and Yu. D. Chashechkin, "Generation of dissipation-gravity waves during thermal convection in a stratified medium," *Prikl. Mekh. Tekh. Fiz.*, No. 3, 49–55 (1991).
8. L. D. Boyer, P. A. Davies, H. J. S. Fernando, and X. Zhang, "Linearly stratified flow past a horizontal circular cylinder," *Philos. Trans. R. Soc. London*, **A328**, 501–528 (1989).
9. W. J. Miles, "On the stability of heterogeneous shear flows," *J. Fluid Mech.*, **10**, 496–508 (1961).
10. I. P. Castro and W. H. Snyder, "Upstream motions in stratified flow," *J. Fluid Mech.*, **187**, 487–506 (1988).
11. L. V. Ovsyannikov, N. I. Makarenko, V. I. Nalimov, et al., *Nonlinear Problems of the Theory of Surface and Internal Waves* [in Russian], Nauka, Novosibirsk (1985).
12. V. I. Bukreev and N. V. Gavrilov, "Perturbations ahead of a wing moving in a stratified fluid," *Prikl. Mekh. Tekh. Fiz.*, **2**, 102–105 (1990).